Impacts of Cathode Current Density on Cathode Wear

Guorong Cao[1], Hao Zhang[2] and Evan Andrews[3]
1. Technical Services and Assurance, Principal advisor – Cell Design
2. Technical Services and Assurance, Manager – Smelting Technical Development
3. Boyne Smelters Limited (BSL), Technical and Growth Manager
Rio Tinto Aluminium Pacific Operations, Brisbane Australia
Corresponding author: guorong.cao@riotinto.com
https://doi.org/10.71659/icsoba2025-al080

Abstract

Cathode wear in aluminum electrolysis cells significantly impacts their efficiency and lifespan. Key drivers of cathode wear rate include cathode current density and metal velocity. Controlling current density and ensuring uniform current distribution across the cathode surface may potentially minimize localized wear. A study was conducted on two Sumitomo S-170 cells at Rio Tinto Aluminium's Boyne Smelters Limited (BSL) to assess whether changing cathode current density distribution can lead to any changes in the pattern of cathode wear. The study involved the trial of hybrid cathode collector bar designs to reduce cathode current density variations. Cell design development and plant trial performances from planned measurement campaigns including physical measurements of cathode wear, have been compared with those of the normal control cells. Detailed results of this proof-of-concept study are presented in this paper.

Keywords: Reduction cell life, Cathode wear, Cathode current density.

1. Introduction

Cathode wear in aluminium electrolysis cells is a critical issue impacting the efficiency and longevity of the cells. The wear mechanisms are complex and influenced by various factors, including the cell design, composition of the cathode material, the electrochemical environment, and operational parameters. One of the causes of cathode wear is the electrochemical reaction between the carbon cathode and the molten aluminium. This reaction leads to the formation of aluminum carbide (Al_4C_3), which can be transported around the cathode surface under the influence of magnetohydrodynamic-driven metal pad flow, causing cathode erosion. Localised high cathode current density may contribute to high wear rate over these cathode areas and lead to uneven wear patterns and shorten cell life. Controlling current density and ensuring uniform current distribution across the cathode surface may potentially minimize localized wear [1].

2. BSL SAS Cell Life Challenges

2.1 BSL Lines1&2 Cell Technology

The original potroom technology at BSL lines 1&2 is the Sumitomo S-170 cell, a side-by-side, end-riser prebaked cell that was originally designed for operation at 170–175 kA. Since commissioning in 1982, BSL has made substantial improvements to increase amperage by more than 40 % above nameplate capacity while improving specific power consumption as illustrated in Figure 1. To achieve this:

- The anode length has been increased by 250 mm, culminating in the need for a new rod assembly in 2005, which corrected the asymmetry of the anode on the rod and increased stub diameter.

- The alumina feeding system has been improved by replacing the centre feed "bar breaker" technology with point feeders in 1989 and installing an automatic alumina distribution system (AADS) to individual cells in 2011.
- Rio Tinto has also developed and implemented many generations of cell lining designs to improve productivity, efficiency and cell life. The existing low energy 4A cell design was validated in early 2015 and fully implemented in 2018.
- A compensation loop was installed on Line 2 in 2013 to further increase Line 2 amperage and reduce specific-energy consumption.
- A magnetically compensated bus bar upgrade (consisting of Under Cell Busbars (UCB) and side risers) was carried out for 53 SAS cells since 2017 [2]. The implementation of UCB cells on Line 2 is planned to continue in 2026.

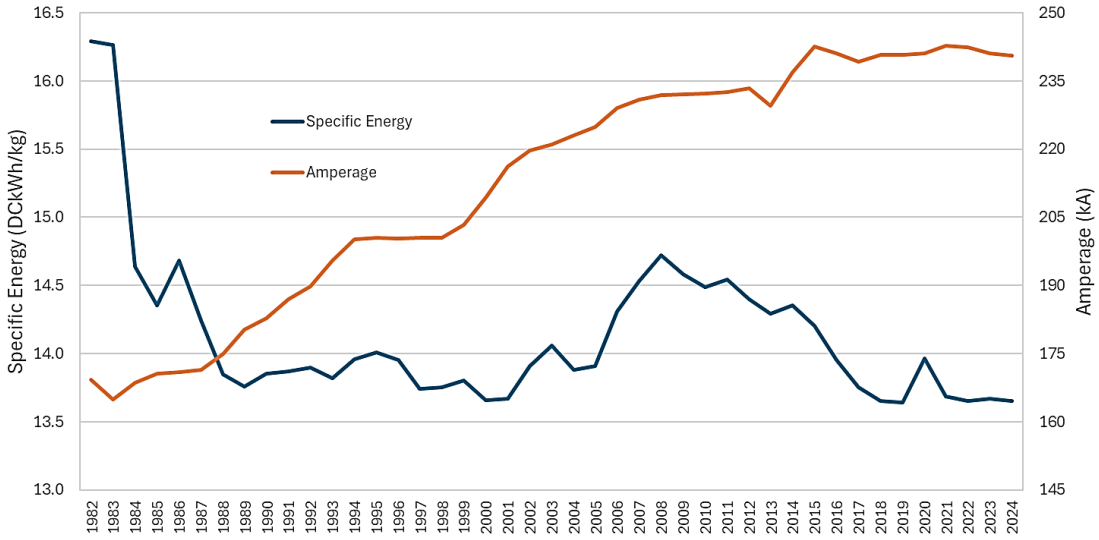

Figure 1. BSL Line 2 amperage and specific energy consumption since commissioning.

2.2 Technical Developments to Improve Cell Life by Reducing Cathode Erosion

Back in 2009, an increasing number of cells at BSL SAS Lines 1&2 were failing 300–500 days earlier than expected. Many of these cells were showing high cathode erosion rates of up to 80 mm/y in the cell corners, with some resulting in the attack of the steel collector bar and "tap-out". Figure 2 shows that the highest cathode erosion occurred in upstream cathode number 2 among the high erosion area between upstream cathodes 1 and 4 during a cell autopsy. Figure 3 shows a typical cathode surface topography for cells that fail through the cathode.

A series of measurement campaigns were carried out to understand the root causes of cathode erosions in order to better understand wear mechanisms and identify potential options to improve cell life. Cathode 'Erosion Map' measurements were carried out using the metal heave/cathode erosion tool (Figure 4). The cathode surface was "mapped" both across its length and width around the area of highest erosion.

Figure 2. Cathode erosion pattern from a cell autopsy showing the highest erosion occurred in upstream cathode number 2 among the high erosion area between upstream cathodes 1 and 4.

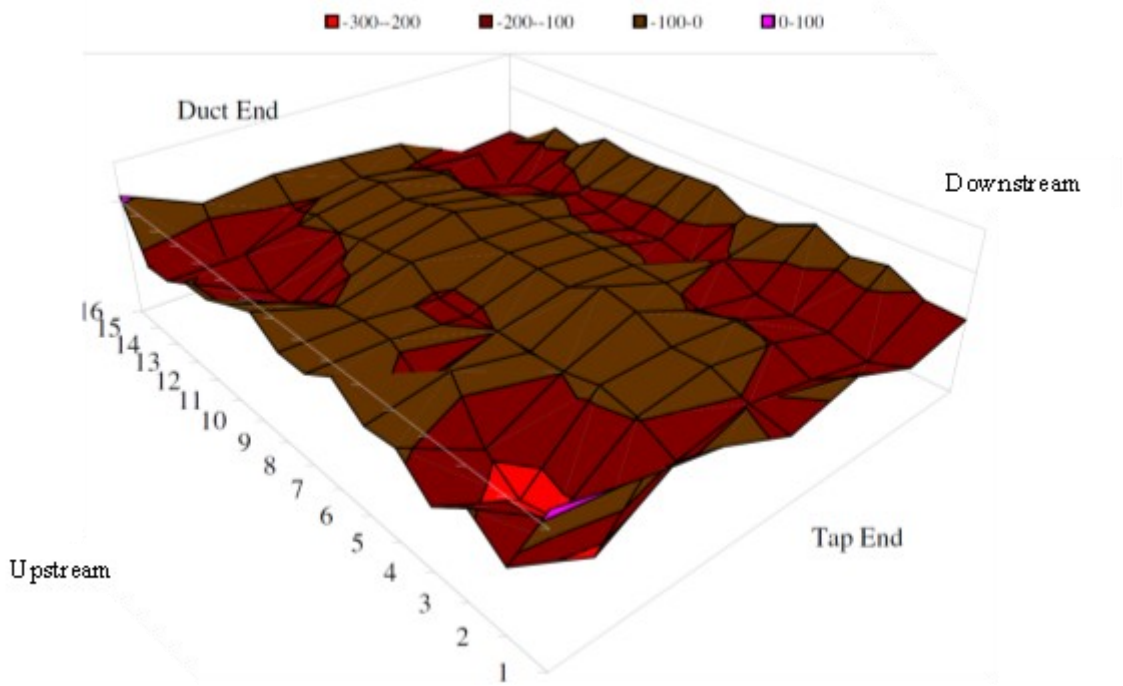

Figure 3. A typical cathode surface topography during a cell autopsy, showing the worst cathode wear occurred in tap end upstream cathodes 1 to 4 (cathode number and erosion in mm).

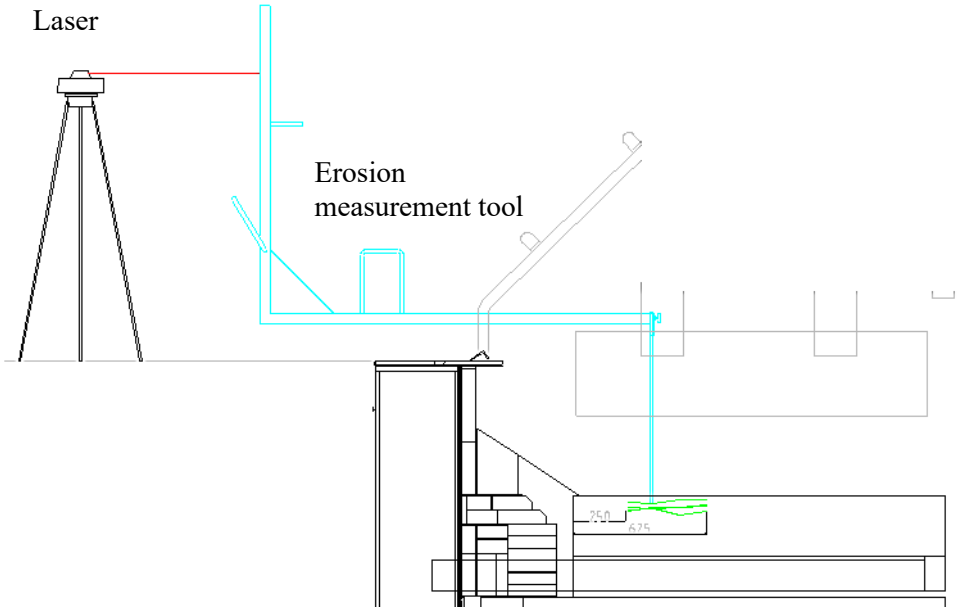

Figure 4. Erosion mapping tools.

Figure 5 shows the 'Etch-a-Sketch' ledge profile tool that was used to measure sidewall ledge 'Erosion Profile'. It is capable to reach approximately 1100 mm in from the cathode edge (corresponds to the centre channel stub location) and to continuously trace the cathode surface through to the sidewall ledge along the centreline of Cathode. Metal velocity, cathode voltage drops, collector bar current density, anode current density and thermal status of the cell were also measured.

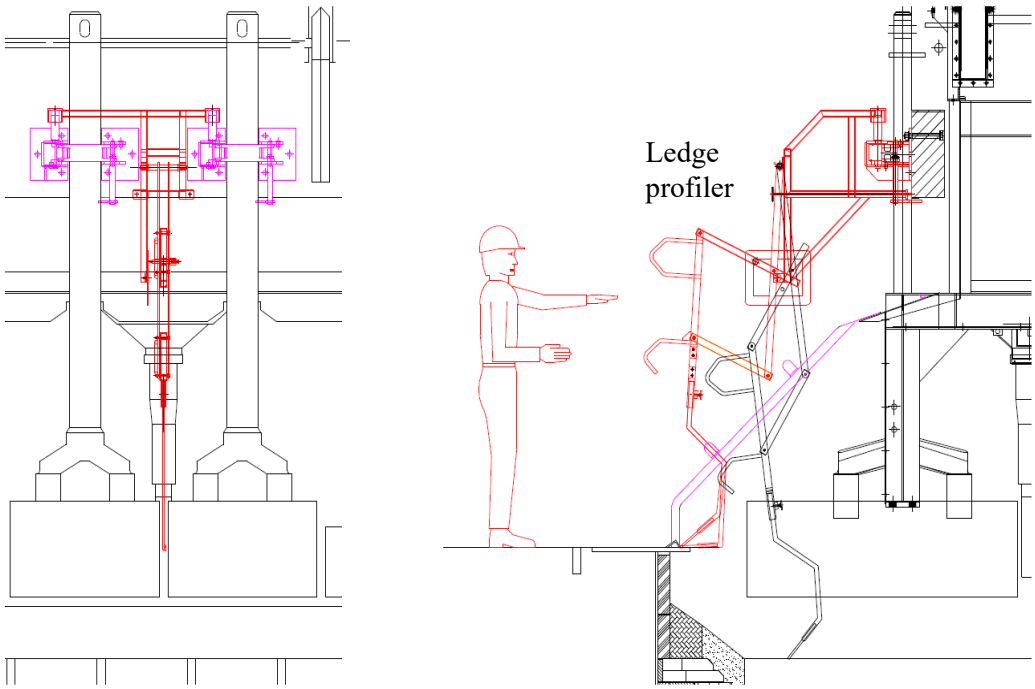

Figure 5. Ledge profiling tool that can reach 1100 mm into the centre of the cathode surface from the cathode edge.

2.3 Key Measurement Results

To understand the measurement results, the average cathode erosion by cell design, normalised to a cell age of 1000 days, is provided in Figure 6 below for comparison.

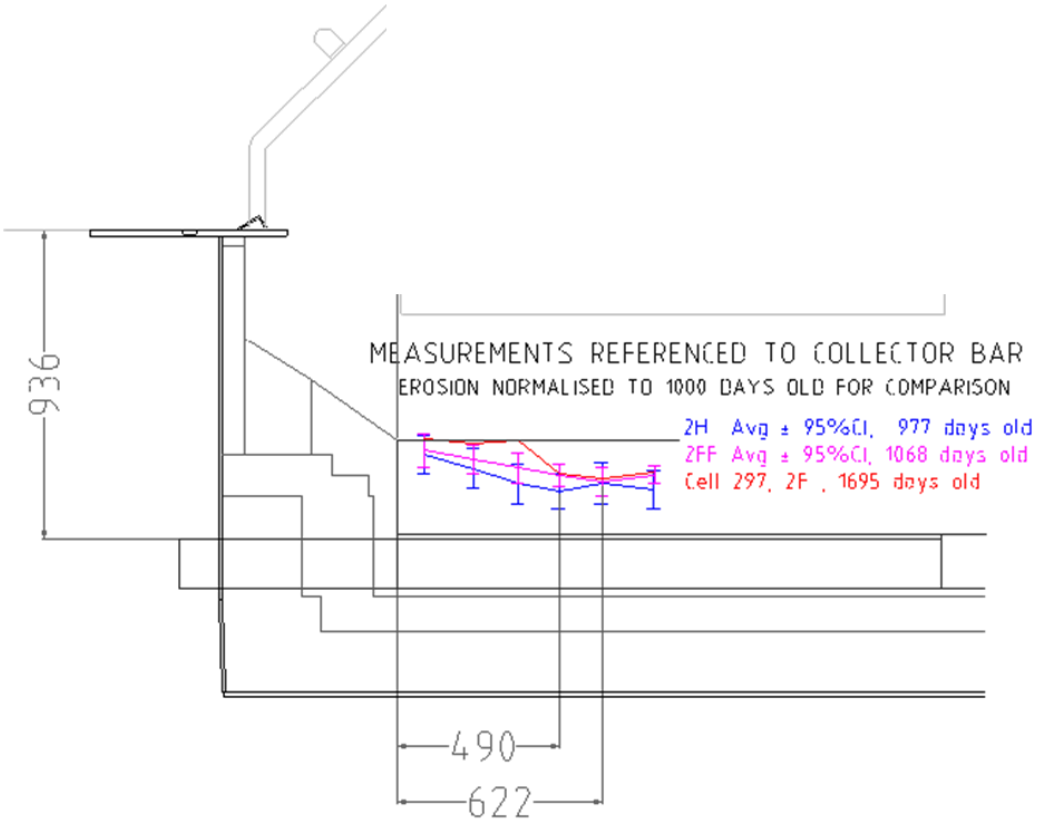

Figure 6. Average cathode erosion by cell design, normalised to cell age of 1000 days for comparison.

Figure 7 shows the measured cathode current draw (CCDs). The CCD results confirmed that the cathode collector bars at the ends always draw higher current than those in the middle.

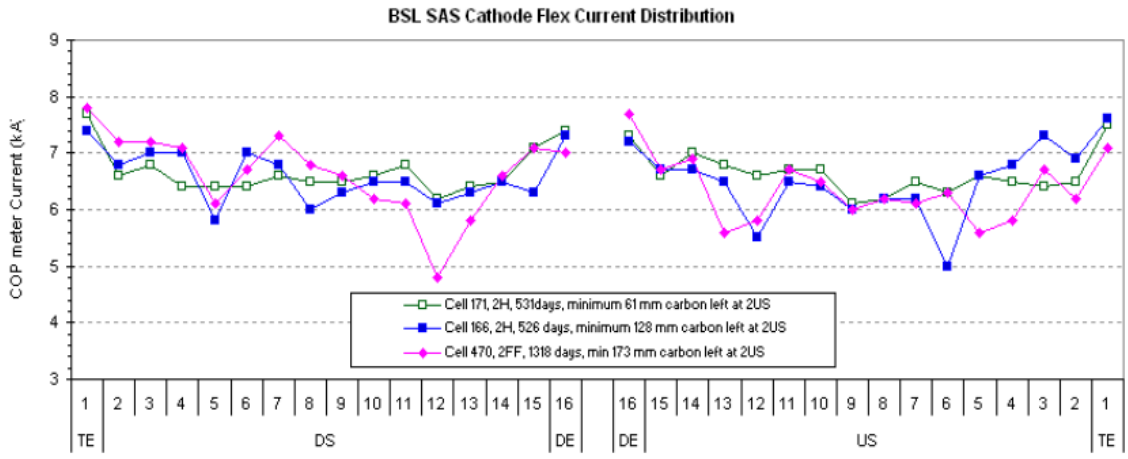

Figure 7. Typical CCD distributions for SAS-170 design. TE= Tap end, DS= Downstream, US= Upstream and DE= Duct End.

To confirm the relationship between metal velocity and the cathode wear pattern, metal velocities in the following two locations in 4 cells were measured using ferrite rods:

1. The first location was between the 10 and 4 stall anodes, in the tap-end upstream corner of the cell, near the area of high cathode erosion and high predicted metal pad velocity.
2. The second location was between the 5 and 17 stall anodes, in the middle downstream side of the cell, near the area of low predicted metal pad velocity.

Figure 8 displays the heavily corroded ferrite rods after 7 minutes immersion in the metal. There is a significant thinning of the section of the rods exposed to molten metal. Figure 9 shows that metal pad velocity generally decreases with increasing metal height. The metal velocity measurements also validated the predicted metal velocity by the MHD model shown in Figure 10.

The higher the concentration of arrows the higher the velocity in the region, from this we can see that bottom right section of the cell experiences the highest velocities. This correlates well with autopsies that show the greatest cathode erosion at the second and third cathodes from the tap end on the upstream side.

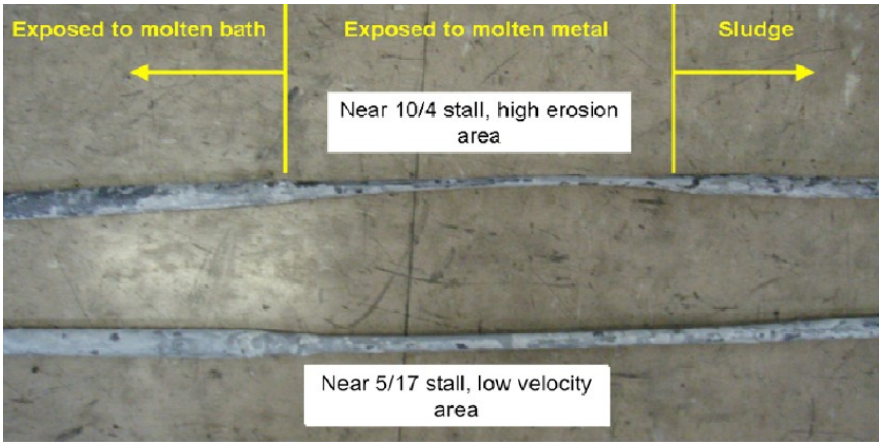

Figure 8. Measured metal velocity with ferrite rods after 7 minutes immersion in the molten aluminium.

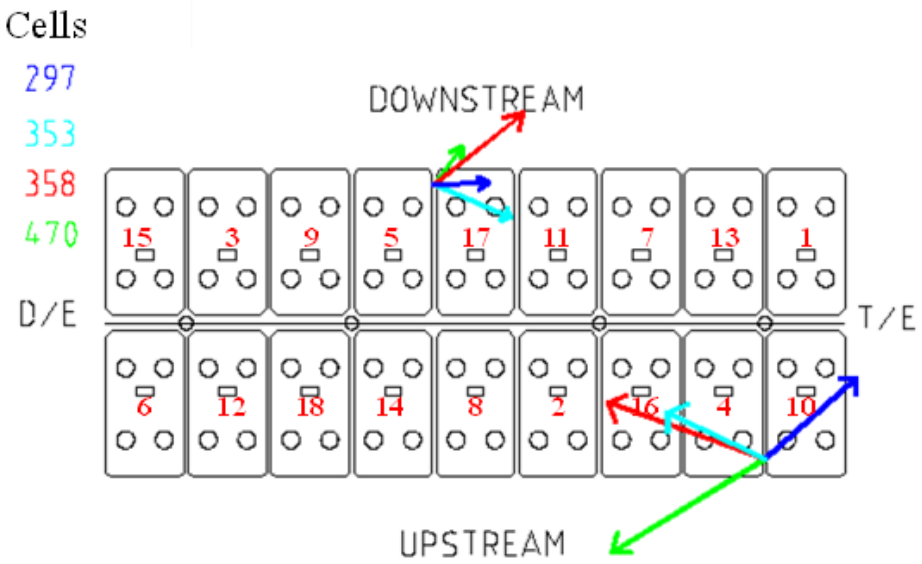

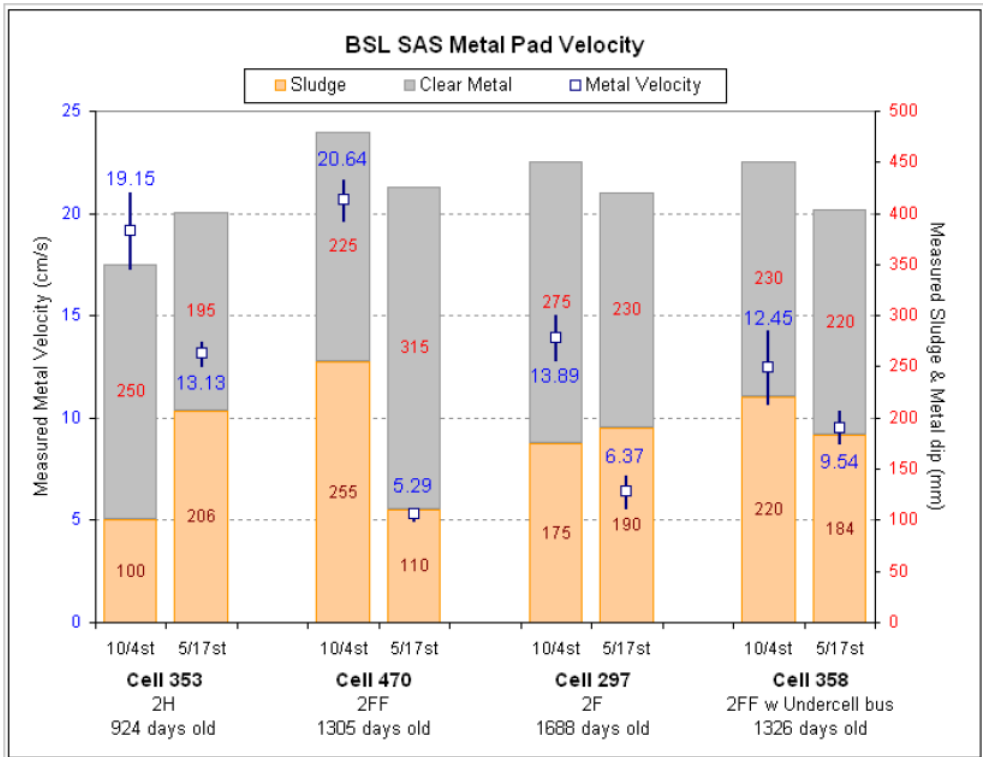

Figure 9. The influence of metal height on metal pad velocity. Top: The measured cells and their metal pad velocity vectors at the downstream and upstream sides, Bottom: The measured velocities confirming the high and low metal pad velocities and the influences of the clear metal height and sludges in the cell.

Downstream

Duct end

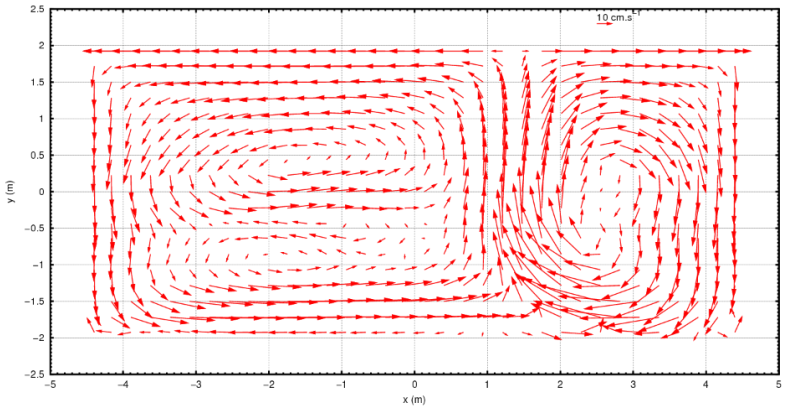

Tap end

Upstream

Figure 10. Model predicted metal velocity.

3. Cathode Design to Improve Cathode Current Distributions and Reduce Cathode Wear

3.1 A Hybrid Cathode Design to Even Out the Cathode Current Density

To assess if the pattern of cathode wear in a S-170 cell is influenced by cathode current draw and hence cathode current density, a hybrid collector bar design with the aim of reducing the amount of current draw in the high wear areas of the cell (Figure 11) was proposed. This was achieved

using copper inserts in the collector bars in the center 8 cathodes of the cell, with the last 4 cathodes on either end installed with traditional collector bars without Cu inserts. Two trial cells were constructed and started in the line 1 booster section (cell 190 and 195) during 2010 at an amperage of 235 kA. The objective of the trial is to assess if evening out cathode current draw can lead to a change in the cathode wear pattern and potentially lead to better cell life. The target cell life improvement was 180 days.

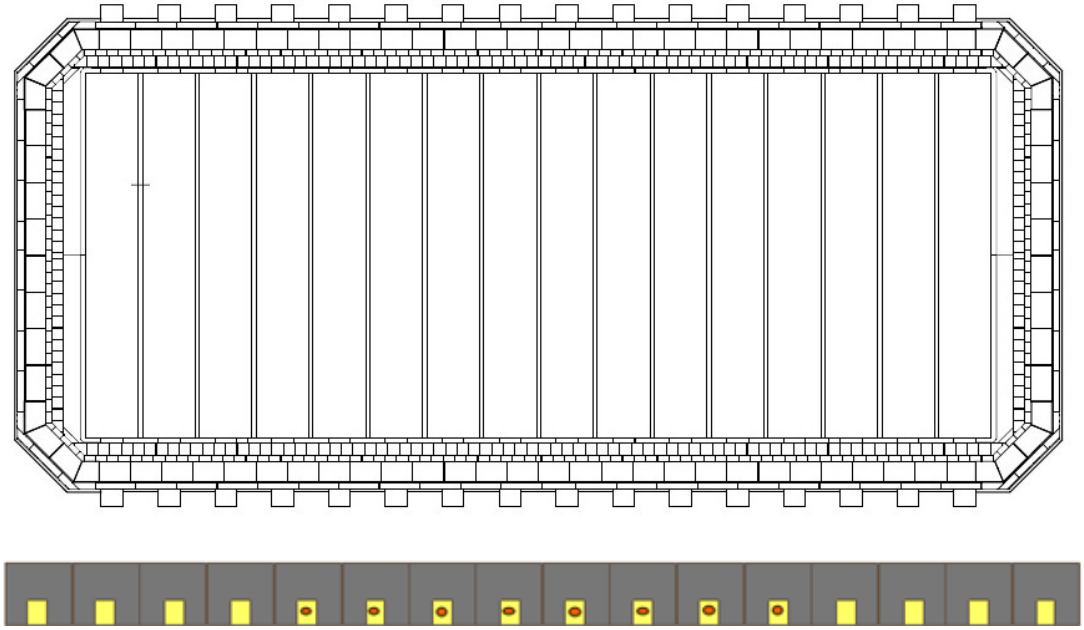

Figure 11. A sketch for the hybrid cathode design.

Control cells with standard collector bars were paired off with the two test cells, so direct comparisons could be made for cells of similar operating age and amperage.

3.2 Measurements to Validate the Trial Cell Performances

A measurement campaign was conducted around 150 days after the trial cells were started to assess the thermal and electrical performances of these two test cells.

Figure 12 shows collector bar current distributions of trial cells versus control cells. There was a statistically significant increase in current draw through the copper containing collector bars. As a result of the increased current draw of the copper bars there was a significant drop in current draw through the end cathodes that was prone to higher erosion rates. The Current draw through the centre 8 copper containing collector bars was 28 % higher than non-copper bars and 16 % higher than the same location on a standard cell.

Cathode voltage drops (CVD) around 150 days were also measured and shown in Figure 13. The red line on Figure 13 represents the average cathode voltage drop for three control cells around the same age. Results for the first copper cell (190) are in blue and the second copper cell (195) in green. For the trial cells, the CVD was around 40 mV lower than control cells. It should be noted that cell 195 experienced significant operational issues and the increase in CVD with age during early life was believed to be related to the operation issues.

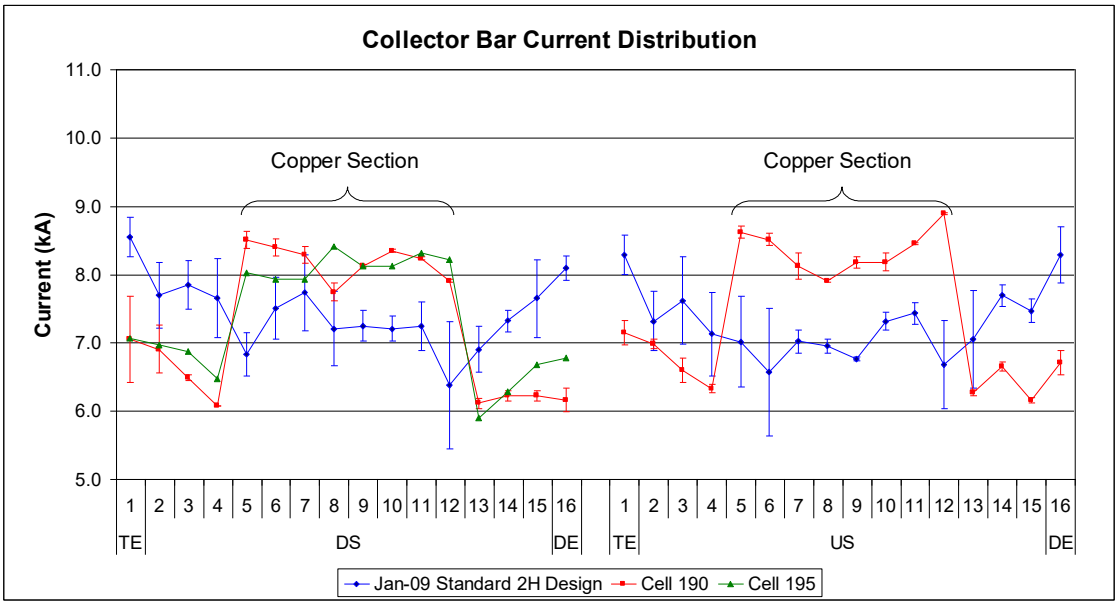

Figure 12. Collector bar current distributions in the trial cells.

It was projected at that time that if all the collector bars were converted to Cu-cored collector bars, the potential CVD benefit might be in the range of 70–80 mV. The actual CVD benefit on fully converted 4 A design cells (with all copper cored collector bars) since 2015 was more than 100 mV. The better CVD saving achieved on the 4 A design cells is believed to be due to the improved heat balance because of the lining upgrade for the 4 A cells.

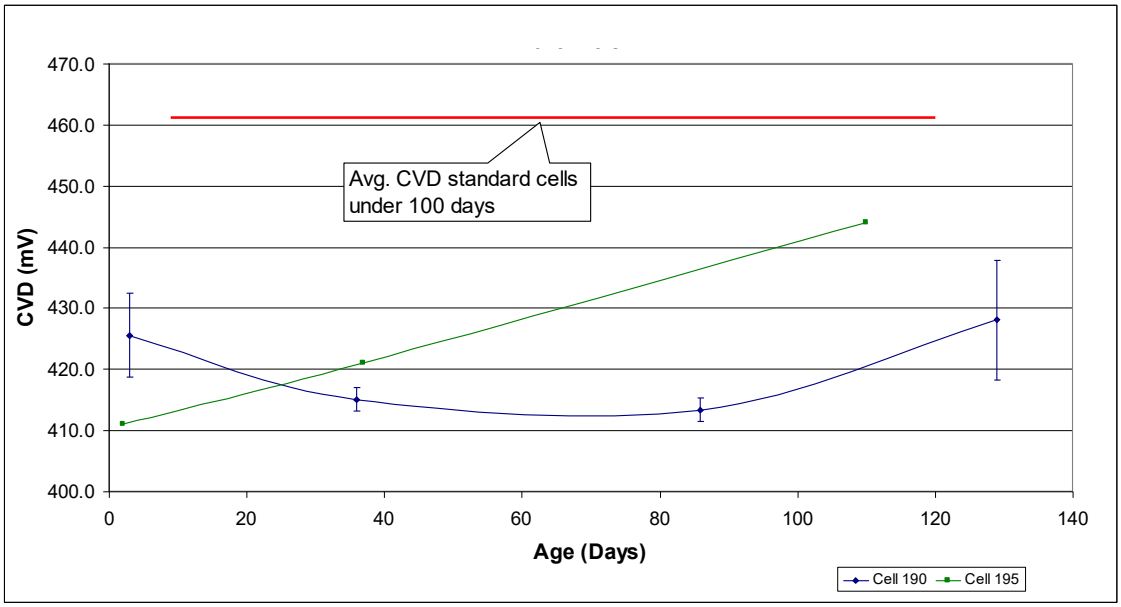

Figure 13. Cathode voltage drops in the trial cells compared with that of the control cells.

One of the primary concerns of the mixed collector bar design was the effects of increased horizontal current flows on metal pad stability. Figure 14 is a simplified illustration of the possible change in current flow experienced in the transition zone between copper and non-copper cathodes.

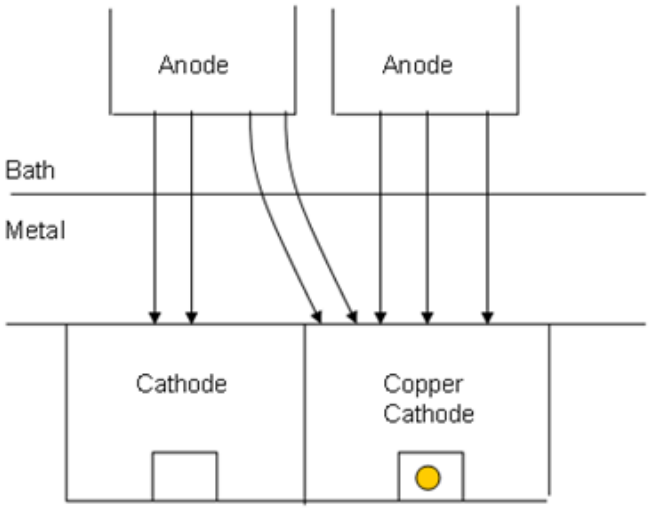

Figure 14. Potential impact of copper on current flow.

Figures 15 and16 display the average daily metal pad noise for cell 190 and 195 versus the average of the three booster group cells (182, 188 and 189). The high noise experience in the first 30 days of operation for cell 190 has been attributed to sludge deposits on the cathode surface and an incorrect anode profile.

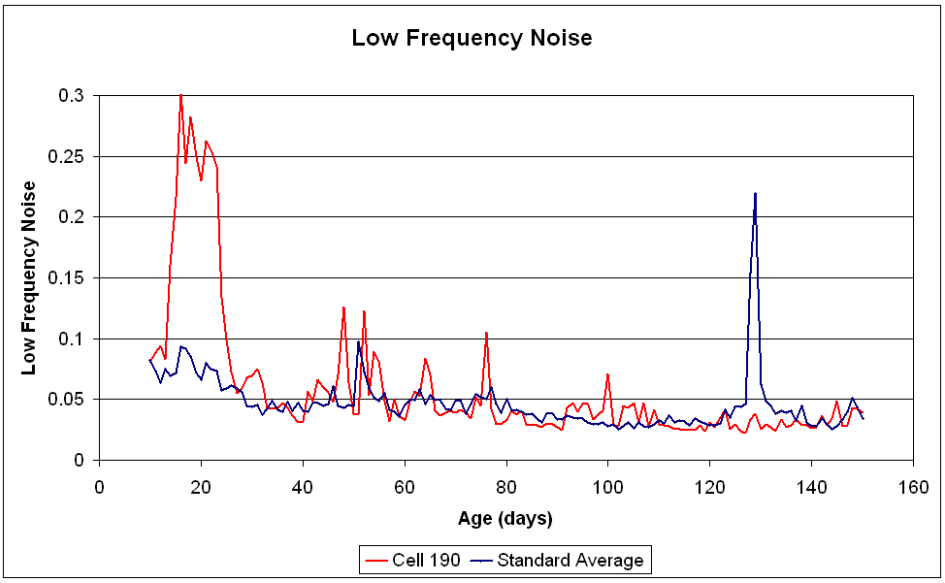

Figure 15. Low frequency noise cell 190.

It can be seen from Figures 15 and 16 that metal pad noise for cell 190 was in general comparable to standard cell and cell 195 was much worse than standard cell. The poor stability observed on cell 195 was believed to be due to process/operational issues.

Metal pad velocity measurements were performed on the two trial cells and two control cells. Figure 17 shows the metal velocities measured for the two trial cells and two control cells. The arrows in the figure represent the metal velocity vectors for each of the measurements. Working from the top right circle to the bottom left circle the following comparisons can be made:

- Metal velocity and direction in downstream tap end (non-copper) are very similar for copper and non-copper designs.

- Velocity is slightly higher (2–3 cm/s) for copper section in upstream duct end. This is approximately the location of the change between copper and non-copper collector bars, which might be contributing to the difference. This location is typically not an area of high erosion.
- On average no difference in upstream copper collector bar cathodes (between anodes 18 and 14), with cell 195 and 190 showing higher and lower velocities than a standard cell.
- Velocities at the upstream duct end (6/12 stall non-copper section) – typically a high velocity area – were slower for the copper cell than the non-copper cell.

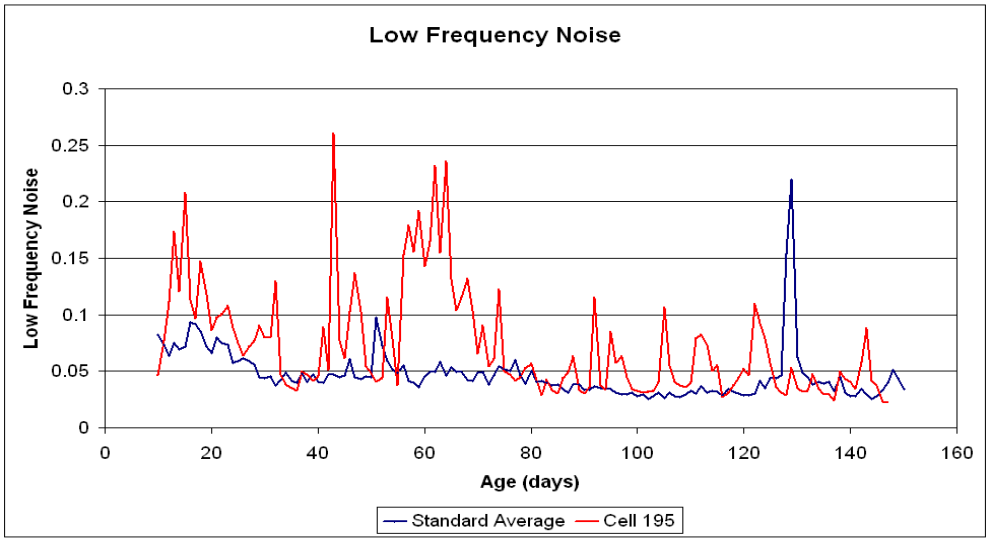

Figure 16. Low frequency noise cell 195.

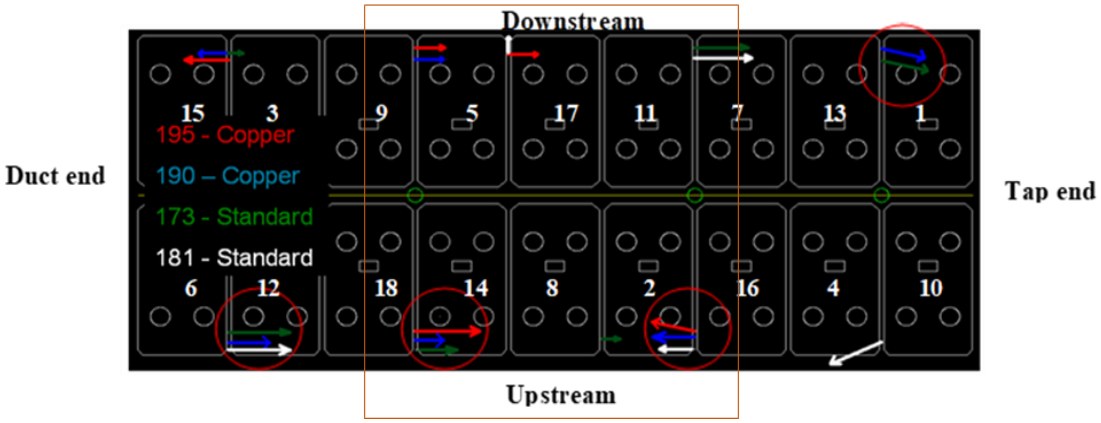

Figure 17. Measured metal velocities (copper section inside the brown shape).

4. Planned Cell Autopsies to Investigate the Impact on Cathode Wear

4.1 Autopsy of the First Trial Cell - Cell 190

The first trial cell was cell 190 and the planned cathode surface autopsy was conducted after 448 days of operation to determine the success of the design on modifying the wear pattern of the cell. Cathode surface topology was surveyed across the entire cell, along with a damage map and photographs of the cell surface. Figure 18 shows an overview of the cell wear pattern and damage observed on the cathode surface. Figure 19 shows a 3D surface topography of the cathode surface.

Significant cathode erosions were present on the upstream side of the cell. The excavation damage through the centre of cathodes #5 and #6 was excluded from these measurements.

The wear pattern indicated significant wear in the typical upstream corners from cathode #1 to #5 and to a lesser degree from cathode #11 to #16. The highest wear measured was on cathode #12 upstream with 129 mm of wear recorded (or 105 mm/year). The wear pattern on cell 190 extended to include the first copper collector bar cathode (cathode 5 and 12). Figure 20 shows the changes in cathode current draws for cell 190 and 195 compared to standard cells. The substantial cathode current draw reduction achieved over the end cathodes for cell 190 and 195 did not reduce the erosion in the traditional high wear areas in upstream tap end cathode (1 to 4) corners. Furthermore, the high wear area has extended to the first cathodes with Cu bar, with the maximum wear on the first copper collector bar cathode from the duct end, upstream side.

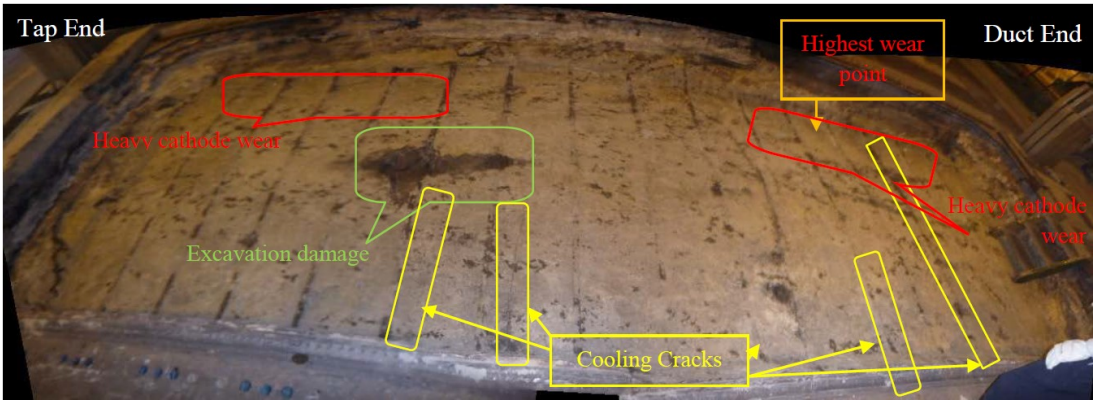

Figure 18. The cell wear pattern and damage observed on the cathode surface on cell 190.

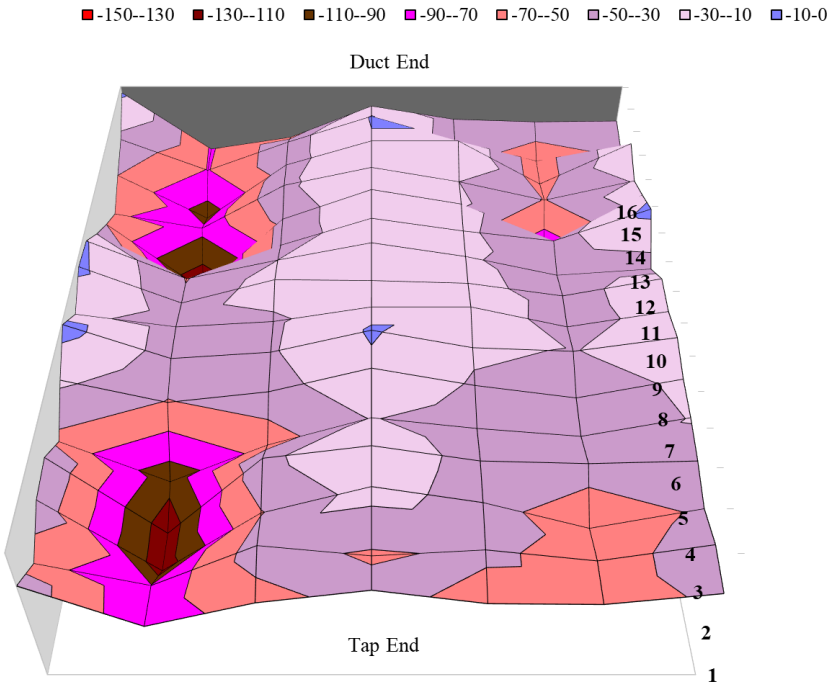

Figure 19. Cathode surface topography of cell 190 during planned autopsy after 448 days after the start up (upstream is on the left side, erosion in mm).

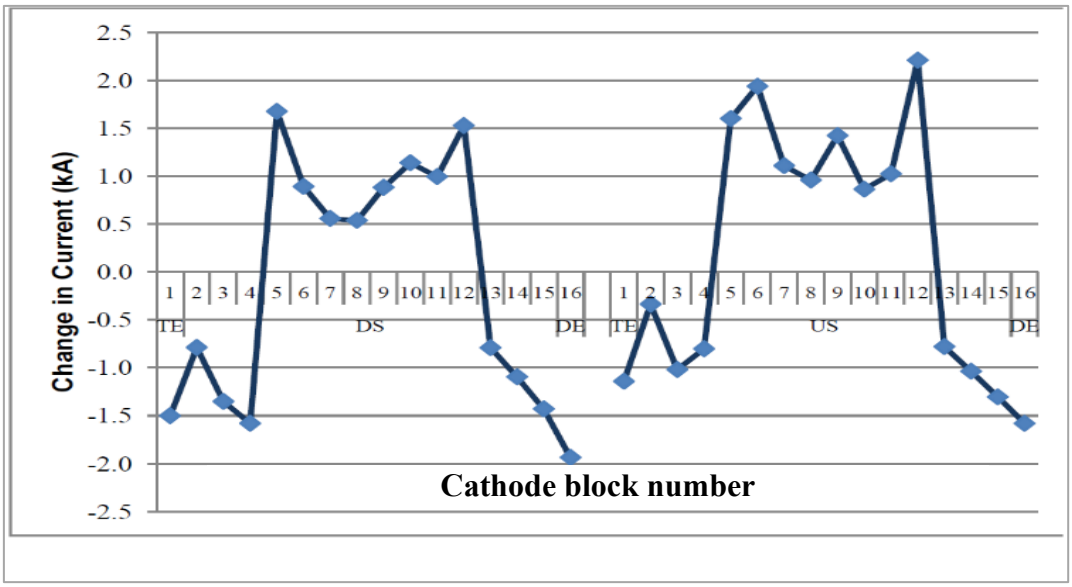

Figure 20. Change in collector current draw in the two hybrid trial cells compared to the standard control cells.

4.2 Autopsy of the Second Trial Cell - Cell 195

The planned autopsy of the second trial cell was conducted after 468 days of operation. Figure 21 shows the cathode surface topography of the second cell again revealing a maximum cathode erosion rate of 90 mm/year (less than the first trial cell at 105 mm/year) in cathode 3 on the tap end upstream side of the cell. However, no significant cathode erosion in the copper to non-copper cathode transition areas was observed as opposed to what was observed on cell 190.

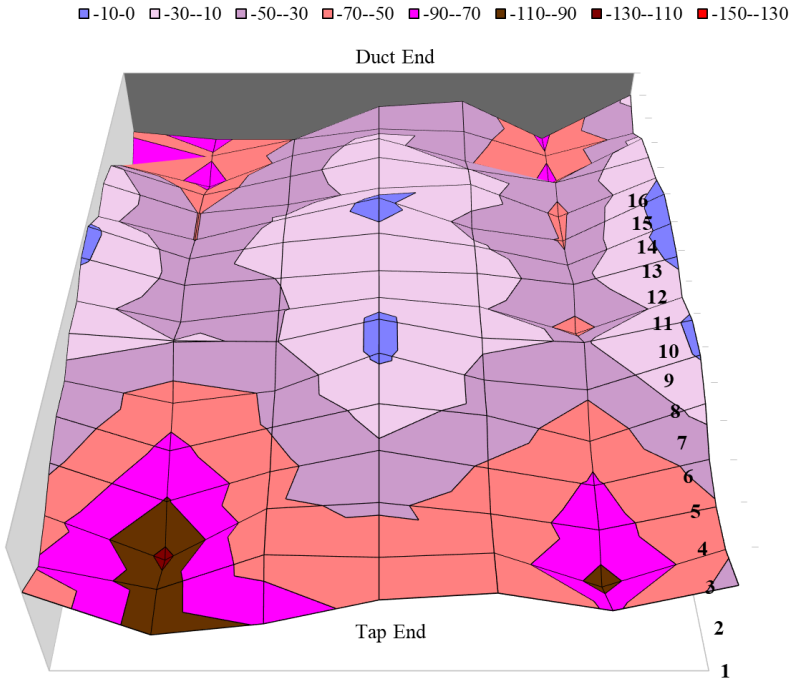

Figure 21. Cathode surface topography of cell 195 during planned autopsy after 468 days after the start up (upstream is on the left side, erosion in mm).

4.3 Restart of Trial Cells and End of Life Autopsy Results

Both trial cells were restarted after planned autopsies around 450 days. Cell 190 lasted another 1708 days with two collector bars cut six months prior to failure, making the total cell life of 2156 days compared to the line average cell life of 1510 days. The cell life achieved for cell 190 was comparable to the longest cell life of 2109 day achieved for the 2H design at that time. Cell 195 Unfortunately tapped out from the sidewall 18 days after the restart due to infiltration through a crack in the sidewall ram fillet.

Figure 22. shows the cathode surface topography taken during the autopsy of cell 190 at the end of its life. The maximum cathode erosion rate is 59 mm/year based on the measurement. The wear rate may be higher (about 65 mm per year) if the full cathode life is assumed to be reached at the time when collector bars were cut (six months shorter than the actual cell life). Figure 23 shows the maximum cathode wear rate at different cell ages for cell 190 in comparison with other cell designs. Maximum cathode wear rates have not shown any noticeable improvement despite a longer cell life. As shown in Figure 23, the maximum cathode erosion rate for the non-copper 2H, 2F, and 2FF design cells decreases with increasing cathode age. This is consistent with the cathode maximum wear rate measured on cell 190. This trend may be related to the harsh operating environment during cell start-up, particularly during gas bake, when some degree of cathode oxidation would inevitably occur. The lower metal level target for young cells might also contribute to the higher wear rate during early life. Another possible reason for the erosion rate decrease with age could be that the eroded area might be filled with mobile sludge, thus protecting the already eroded area from further erosion.

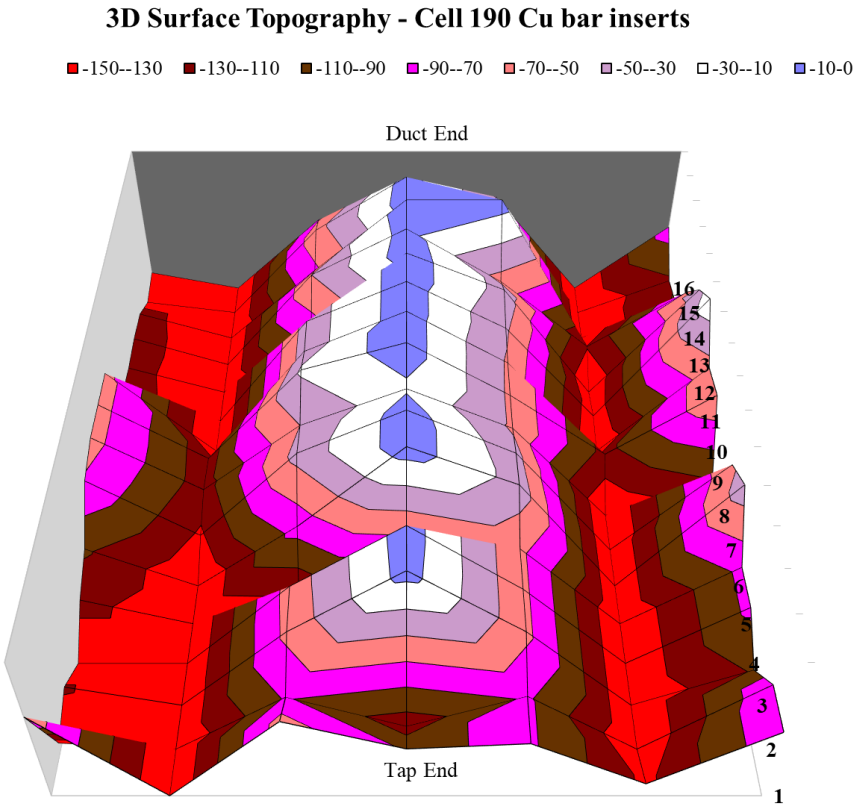

Figure 22. Cathode surface topography of cell 190 obtained during final autopsy after total of 2156 days cell operation (upstream is on the left side, erosion in mm).

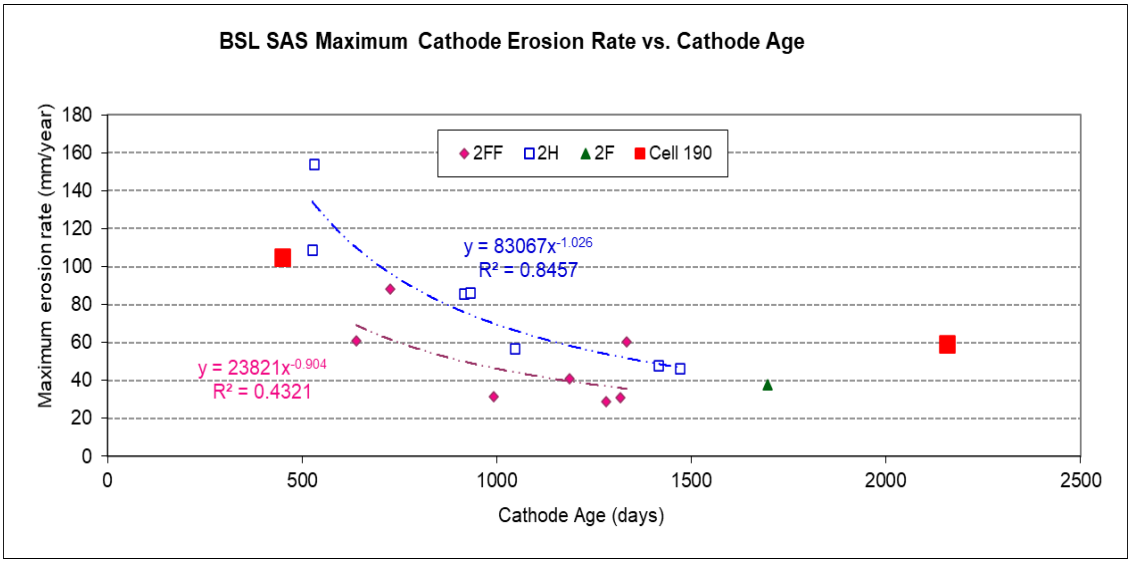

Figure 23. A comparison of cathode wear rate of cell 190 with other designs.

5. Discussion and Conclusions

A "proof of concept" technical trial has been conducted to assess if the cathode wear pattern can be influenced by using a hybrid cathode design to even out cathode current density in the end riser S-170 cell with no magnetic compensation. The use of copper in the middle cathodes was found to be successful in redirecting more than 20 % current from the end cathodes towards the centre cathodes. However, it did not result in any significant change in cathode wear patterns as well as the maximum cathode wear rate. This implies that the cathode wear mechanism for S-170 technology is very complex and unlikely to be caused by any single mechanism [4]. Varying cathode current density itself was not sufficient for altering either the cathode wear pattern or the magnitude of cathode wear. MHD related wear mechanism is believed to play a major role in the wear pattern of S-170 cells because no significant improvements in metal velocity and metal pad stability were achieved in the trial cells.

Despite the fact that one out of the two trial cells achieved a record cell life with a 40 % cell life increase compared to the average cell life of standard cells during the same period, its cathode wear pattern and maximum wear rate remained high. Eventually, the project team chose to pursue alternative designs to improve energy efficiency and cell life, including busbar modifications to address the root cause of the significant cathode wear [3]. These cell design changes have proven to be highly successful, with the average cell life now at BSL L12 close to 2000 days as opposed to 1500 days back in 2015.

6. Acknowledgement

The authors wish to acknowledge all the staff from the Reduction team at the former Pacific Technology Centre of Rio Tinto Aluminium and BSL for their contribution to the project work. In particular, Tseng Khoo, David Clark and Chris Johnston from the former Pacific Technology Centre were instrumental in the execution of the project.

7. References

1. Arne P. Ratvik, Samuel Senanu, Zhaohui Wang, Tor Grande, Understanding cathode wear, *Proceedings of the 12th Australasian Aluminium Smelting Technology Conference*, 2nd-7th December 2018, Queenstown, New Zealand, 568–573.

2. Sen Zhou et al., Numerical simulations of copper rod insertion effects on current density, flow field distribution, cathode wear, and electrothermal dynamics in aluminum reduction cells, *Light Metals* 2025, 518–525. https://doi.org/10.1007/978-3-031-80676-6_67
3. Chris Corby et al., Modernisation of Sumitomo S170 cells at Boyne Smelters Limited, *Light Metals* 2019, 543–552. https://doi.org/10.1007/978-3-030-05864-7_69
4. M. Johnston et al., Understanding cathode erosion, *CRC/REP/96/054*, CRC, 15th October 1996.